

**The MODIFIED COMPRESSION FIELD THEORY: THEN AND NOW**

Vahid Sadeghian and Frank Vecchio

**Abstract:** The Modified Compression Field Theory (MCFT) was introduced almost 40 years ago as a simple and effective model for calculating the response of reinforced concrete elements under general loading conditions with particular focus on shear. The model was based on a smeared rotating crack concept, and treated cracked reinforced concrete as a new orthotropic material with unique constitutive relationships. An extension of MCFT, known as the Disturbed Stress Field Model (DSFM), was later developed which removed some restrictions and increased the accuracy of the method. The MCFT has been adapted to various types of finite element analysis programs as well as structural design codes. In recent years, the application of the method has been extended to more advanced research areas including extreme loading conditions, stochastic analysis, fiber-reinforced concrete, repaired structures, multi-scale analysis, and hybrid simulation. This paper presents a brief overview of the original formulation and its evolution over the last three decades. In addition, the adaptation of the method to advanced research areas are discussed. It is concluded that the MCFT remains a viable and effective model, whose value lies in its simple yet versatile formulation which enables it to serve as a foundation for accurately solving many diverse and complex problems pertaining to reinforced concrete structures.

**Keywords:** nonlinear analysis; reinforced concrete; shear behavior

**Biography:**

**Vahid Sadeghian** is a PhD graduate at the Department of Civil Engineering at the University of Toronto. His research interests include hybrid (experimental-numerical) simulation, multi-platform analysis of reinforced concrete structures, and performance assessment of repaired structures.

**Frank J. Vecchio**, FACI, is a Professor at the Department of Civil Engineering at the University of Toronto. He is a member of Joint ACI-ASCE Committees 441, Reinforced Concrete Columns, and 447, Finite Element Analysis of Reinforced Concrete Structures. His research interests include nonlinear analysis and design of reinforced concrete structures, constitutive modeling, performance assessment and forensic investigation, and repair and rehabilitation of structures.

## INTRODUCTION

### Lessons Learned from Shear Failures

Predicting the shear behavior of reinforced concrete (RC) structures is a crucial and challenging task which has not been fully solved yet. Over the last few decades, underestimating the complexity of the problem and relying on limited knowledge of shear behavior have led to several catastrophic failures. Some of the more recognized shear failures, and the resulting experimental investigations that greatly improved our understanding of the behavior of concrete in shear, are summarized in the following.

The basis for shear design provisions of most current codes is a truss model developed by Mörsh (1909) more than a century ago. In this model, the compression component of the shear load is carried by concrete struts, while the tension component is carried by longitudinal and transverse reinforcement. In 1955, the shear failure of a US Air Force warehouse raised questions about the accuracy of such shear design provisions. The experimental investigations that followed demonstrated the detrimental effect of axial tensile force on the shear strength of lightly reinforced members (Elstner and Hognestad, 1957). Later, Bhide and Collins (1989) tested 24 panel elements under combined shear and tension and concluded that the reduction in shear capacity was influenced by the amount and distribution of the longitudinal reinforcement. For members containing sufficient longitudinal reinforcement, this reduction was much less than in members with no tension reinforcement. Based on a review of previous experimental studies, Collins and Kuchma (1999) demonstrated that the failure of the US Air Force warehouse was mainly due to the size effect in shear, rather than the influence of axial tensile force. One of the most well-known test programs to investigate shear behavior was conducted by Kani et al. (1979) which included examining the response of more than 300 specimens. The experimental findings resulted in development of new shear design equations that were included in the ACI code (1971) and mostly remain unchanged to date. In 1991, the collapse of the Sleipner A offshore platform, the most expensive shear failure in history with a total economic loss of about \$700 million, and the resulting experimental investigation conducted by Gupta (2001) indicated that the beneficial effects of the axial compression force on the shear strength had been seriously overestimated and was among the factors contributing to the failure. It was concluded that the shear design provisions of ACI code for structures with high axial load or prestressed structures can be unsafe. While the problem of shear behavior was assumed to be nearly solved in recent years, the collapse of the Laval bridge in 2006, caused by shear failure of a 1.25 m (49.21 in.) thick reinforced concrete slab, showed that it is still too early to draw such a conclusion. The experimental tests conducted by Sherwood et al. (2007) on shear-critical slab-strip specimens indicated the importance of accurately considering the size effect and aggregate interlock in predicting shear behavior. Collins et al. (2008) compared the observed failure loads of these specimens against the failure loads calculated using Canadian, American, European, and British design codes. There were considerable inconsistencies between predictions of the four design codes particularly with variation in the specimen depth or addition of stirrups. Collins et al. (2015) further investigated the size effect by testing a very deep slab specimen under an off-center point load. To assess the ability of existing analysis and design procedures, prior to the test, 66 engineers were invited to predict the failure loads of the two shear spans. It was concluded that the failure load of the shear span with no shear reinforcement was dangerously overestimated by many engineers. The ‘size effect’, and the divergent behavior between narrow deep elements (beams) versus wide shallow elements (slabs), remain contentious issues.

### Analytical Models for Shear Behavior

The aforementioned catastrophic shear failures, and many others, have inspired engineers to develop progressively more refined analytical models over the years. The Mörsh truss model assumed that the inclination of the concrete compression struts was constant and equal to 45 degrees, a simplification that was later found to be incorrect. Hence, modified truss models were proposed with variable angle of inclinations. These models were further improved by considering the contributions of the concrete to the shear strength in the form of residual tensile strength and aggregate

interlock at the crack surface. The application of truss models was extended to non-yielding domains by using the theory of plasticity. In addition, for beams with large span-to-depth ratio where the direct transfer of force by the compression strut is not fully valid, a “tooth model” originally proposed by Kani (1964) was found to be a better representation of the shear behavior. The aforementioned improvements are discussed in detail by the ACI-ASCE Committee 445 (1999). In recent years, more advanced truss models have been developed capable of analyzing other types of shear-critical RC members including walls under cyclic loads (Panagiotou, et al., 2012) and columns with the arch action (Pan and Li, 2013).

The brittle nature of the typical shear failure encouraged many researchers to apply fracture mechanics principles in modeling the shear strength of RC members. Hillerborg et al. (1976) proposed the well-recognized fictitious crack model which represented cracks in a discrete manner and was based on a concrete tensile strength versus crack width relationship. However, the discrete representation of the cracks could not capture the influence of micro-cracking on the shear behavior. Bazant and Gambarova (1984) proposed the crack band model in which the fracture surface consisted of a zone of micro-cracks and the size effect was considered in the energy equation. Van Mier (1996) showed that residual tensile stresses exist within the crack band as a result of a phenomena known as “crack bridging”. In recent years, the application of methods based on fracture mechanics has been extended to other types of loading conditions (e.g., seismic and impact) and other concrete materials (e.g., fiber-reinforced concrete). These advancements are summarized by IA-FraMCoS (2016). However, most fracture mechanics models require assumptions for the crack path and the governing failure mechanism prior to analysis.

In an alternative approach to calculating shear strength, several empirical equations were derived by curve fitting to a series of experimental data. Empirical methods are the basis for the shear design provisions of the American and most European design codes. However, as discussed in detail by Collins et al. (2008), because of the complexity of the shear behavior and the narrow range of test parameters, the application range of an empirical method is typically limited. For a comprehensive representation of situations encountered in practice, models with a more rigorous theoretical basis are required.

One effective rational approach which has attracted considerable interest in recent decades is the Modified Compression Field Theory (MCFT) (Vecchio and Collins, 1986). The MCFT is the refined version of the Compression Field Theory (CFT) (Mitchell and Collins, 1974), a smeared rotating crack model originally developed for analysis of beams in shear and torsion. In both models, the compatibility and equilibrium conditions as well as the stress-strain relationships are formulated in terms of average values of stresses and strains. The CFT assumes that the cracked concrete cannot resist any tension and the shear force is carried by a field of diagonal compression. The inclination of the compression field is determined using an approach similar to that used in the Tension Field Theory (Wagner, 1929) developed for the post-buckling shear resistance of thin metal girders. The MCFT improved the original model by accounting for compressive strength reduction in concrete due transverse cracking, concrete tensile strength after the cracking, and local stress conditions at the crack surface. The MCFT is the basis for the shear design provisions of the Canadian design code (2014) and the AASHTO LRFD Bridge Design Specifications (2014). Vecchio (2000) extended the MCFT and proposed the Disturbed Stress Field Model (DSFM) which removed some of the restrictions and improved the accuracy of the model. **Fig. 1** compares the equilibrium, compatibility and constitutive relationships in the CFT, MCFT, and DSFM models. Bentz et al. (2006) proposed a simplified version of the MCFT that can predict the shear strength of RC elements in a form suitable for inclusion in code applications. In recent years, the application of the MCFT has been extended to more advanced research areas including extreme loading conditions, stochastic analysis, fiber-reinforced concrete, repaired structures, multi-scale analysis, and hybrid simulation.

This paper presents a summary of the MCFT formulation and the adaptation of the model to sectional and finite element analysis methods. The extension of the model to the DSFM and the resulting improvements, as well as the findings of three comprehensive verification studies performed on the MCFT and DSFM models are reviewed. In addition, a comprehensive discussion regarding the application of the model to advanced research areas and related references is provided.

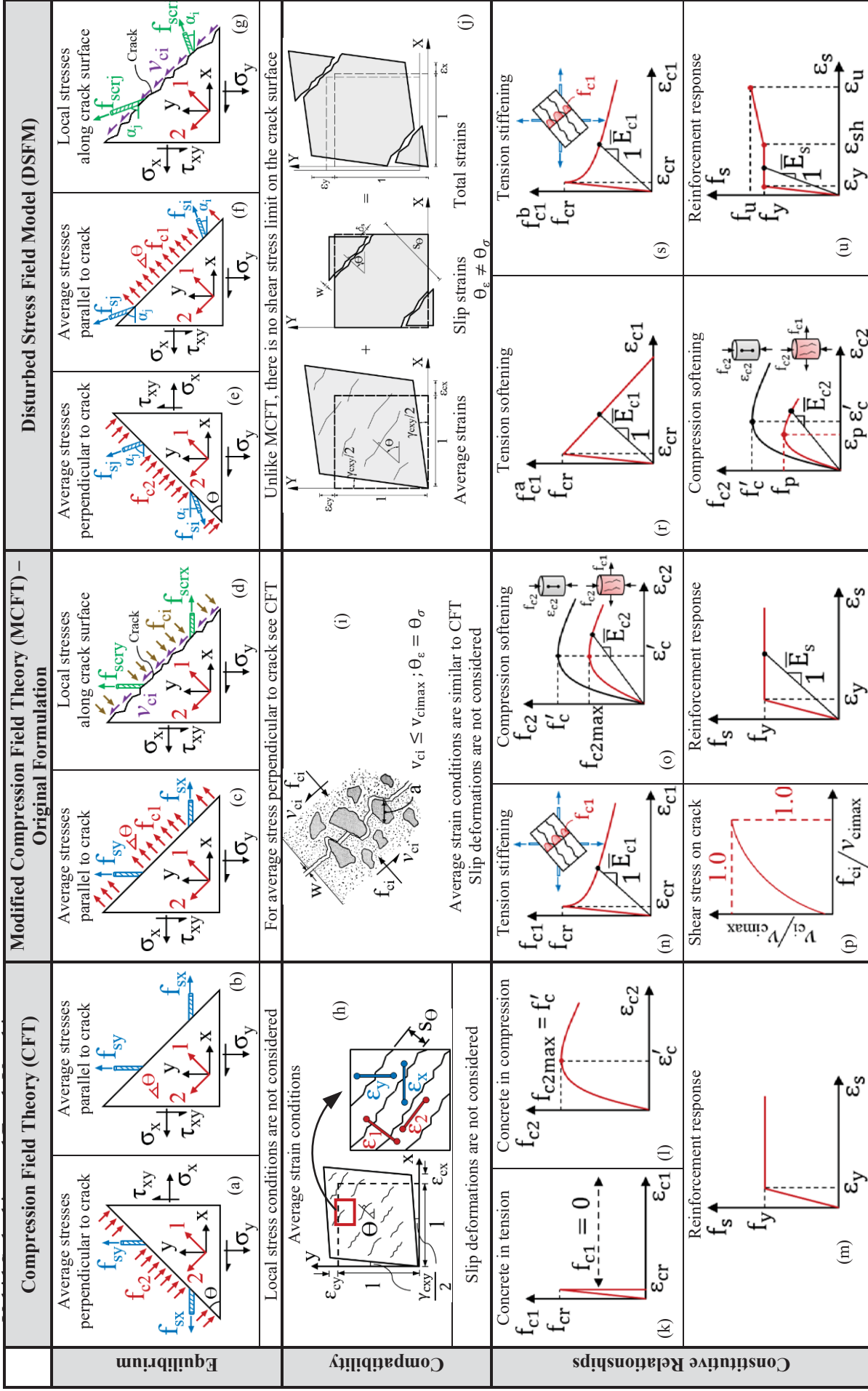
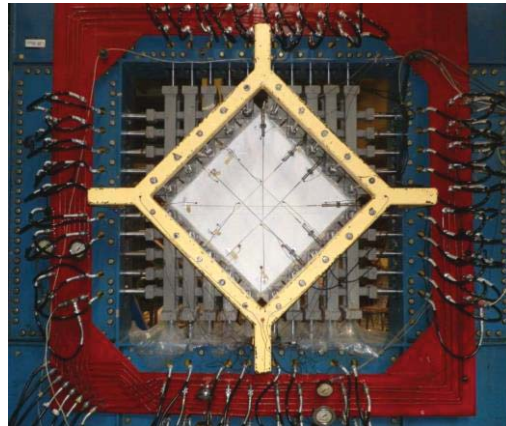


Figure 1 — Comparison between CFT, MCFT, and DSFM models

### THE SHEAR TESTING RIG

The MCFT was calibrated based on the behavior of a large number of reinforced concrete panels tested under well-defined loading conditions using the Panel Element Tester (a.k.a. “The Shear Rig”) at the University of Toronto. This testing facility was the first of its kind in the world, developed in 1979, and has since been emulated by various research laboratories. It enabled the testing of reinforced concrete panel specimens with dimensions of  $890 \times 890 \times 70$  mm ( $35 \times 35 \times 2.75$  in.) under various combinations of in-plane stresses in a monotonic or reversed cyclic manner. The facility is still in use today. Each specimen has 20 shear keys located around its perimeter through which load is applied. As shown in **Fig. 2**, a test specimen is mounted in the Rig with its edges inclined at a 45 degree angle. The loading apparatus consists of 37 hydraulic jacks and 3 rigid links which are oriented in the horizontal and vertical directions. Two of the three rigid links connect at one key creating a pin connection, while the other rigid link acts as a virtual roller. To prevent the specimen from moving in the out-of-plane direction, a lateral support frame is attached to the back of the test setup.

The original test program that contributed to the development of the MCFT included 30 panel specimens. The test variables were the loading conditions, percentage of the transverse and longitudinal reinforcement, and the concrete compressive strength. Details of the test program were provided by Vecchio and Collins (1982). In 1985, an international competition was held to predict the load-deflection responses of four of the panel specimens (Collins et al., 1985). Twenty-seven researchers from 13 different countries participated in the competition. In general, the analytical models overestimated both the ultimate strength and ductility of the test panels. These deficiencies were mainly attributed to neglecting the compressive strength reduction in concrete due to transverse cracking (i.e., compression softening) and underestimating the tensile strength of concrete after cracking (i.e., tension softening). Based on the panel test results, new stress-strain relationships for concrete were developed which later were used in the MCFT formulation. Since then, the formulations have been verified by more than 200 tests of RC panel elements. In more recent years, the Shear Rig has been employed to investigate the behavior of fiber-reinforced concrete (FRC) elements. Based on the test results, new FRC material models were developed and incorporated in the MCFT formulation.



**Figure 2 — RC panel specimen mounted in Shear Rig**

### MODIFIED COMPRESSION FIELD THEORY (MCFT)

The MCFT, originally developed by Vecchio and Collins (1986), is a generalized approach for modeling the behavior of reinforced concrete elements. It considers cracked concrete as a unique orthotropic material with its own constitutive relationships. The theory is based on a rotating smeared crack model that treats stresses and strains in an average sense, and allows the crack direction to gradually reorient depending on the material response and loading condition. Special consideration is given to the local stress conditions at the crack surface. A key assumption in the model is that the directions of principal stress and principal strain in the concrete remain coincident. The model is formulated using three sets of equations: equilibrium, compatibility, and constitutive relationships. A brief overview of each set of equations is provided below.

#### **Equilibrium Relations**

**Average stress conditions** — consider a reinforced concrete element containing reinforcement in the X and Y directions. As shown in **Fig. 3**, the equilibrium conditions require that the applied stresses ( $\sigma_x$ ,  $\sigma_y$ ,  $\tau_{xy}$ ) be resisted by average stresses in the concrete ( $f_{cx}$ ,  $f_{cy}$ ,  $v_{cxy}$ ) and average stresses in the reinforcement ( $f_{sx}$ ,  $f_{sy}$ ). Using a Mohr’s circle

of average stresses and assuming no dowel action from the reinforcement, the equilibrium equations can be written as follows:

$$\sigma_x = \rho_x \times f_{sx} + f_{c1} - v_{cxy} \cot \theta_c \quad (1)$$

$$\sigma_y = \rho_y \times f_{sy} + f_{c1} - v_{cxy} \tan \theta_c \quad (2)$$

$$\tau_{xy} = v_{cxy} = \frac{f_{c1} - f_{c2}}{\tan \theta_c + \cot \theta_c} \quad (3)$$

where  $\rho_x$  and  $\rho_y$  are the smeared reinforcement ratios in the X and Y directions,  $f_{c1}$  and  $f_{c2}$  are the principal tensile and principal compressive stresses in concrete, and  $\theta_c$  is the crack inclination. **Fig. 1(a)** and **Fig. 1(c)** show the free body diagrams for the equilibrium equations.

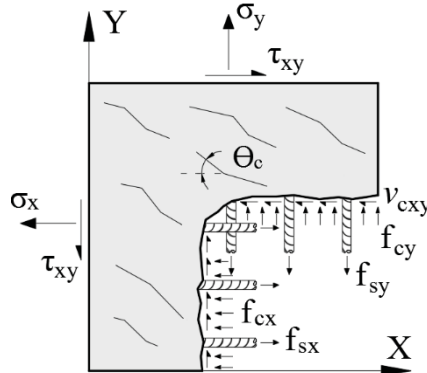


Figure 3 — Concrete element reinforced in X and Y directions

**Local stress conditions** — in cracked reinforced concrete, the tension stiffening mechanism allows the concrete to carry tensile stresses after cracking resulting from bond with the reinforcement. Since the tensile strength of concrete is zero at crack locations, the average tensile stress must be carried across the cracks by local increases in the reinforcement stresses. From equilibrium equations, as shown in **Fig. 1(d)**, the local stresses in the reinforcement ( $f_{sxcr}$ ,  $f_{sy-cr}$ ) at the crack locations can be determined as:

$$f_{sxcr} = \frac{1}{\rho_{sx}} (f_{c1} + f_{ci} + v_{ci} \cot \theta_c + \rho_{sx} f_{sx}) \leq f_{yx} \quad (4)$$

$$f_{sy-cr} = \frac{1}{\rho_{sy}} (f_{c1} + f_{ci} - v_{ci} \tan \theta_c + \rho_{sy} f_{sy}) \leq f_{yy} \quad (5)$$

where  $v_{ci}$  and  $f_{ci}$  are the shear and compressive stresses on the crack surface (see **Fig. 1(i)**). The shear stress is transferred across the crack surface based on the friction mechanism, also known as aggregate interlock. The interface shear stress is calculated from the following equation based on an experimental study conducted by Walraven (1981):

$$v_{ci} = 0.18v_{cimax} + 1.64f_{ci} - 0.82 \frac{f_{ci}^2}{v_{cimax}} \leq v_{cimax} \quad (6)$$

where

$$v_{cimax} = \frac{\sqrt{-f'_c}}{0.31 + \frac{24w}{a + 16}} \quad (7)$$

where  $a$  and  $w$  are the maximum aggregate size and the average crack width in millimeters (1.0 mm = 25.4 in.) and  $f'_c$  is the concrete cylinder compressive strength in MPa (1.0 MPa = 145.0 psi). The average crack width ( $w$ ) is estimated as the product of the principal tensile strain ( $\epsilon_1$ ) and the average crack spacing ( $s_\theta$ ):

$$w = \epsilon_1 s_\theta \quad (8)$$

The average crack spacing ( $s_\theta$ ) is determined from the nominal crack spacings in the X and Y directions ( $s_x$ ,  $s_y$ ) as follows:

$$s_\theta = \frac{1}{\frac{|\sin \theta_c|}{s_x} + \frac{|\cos \theta_c|}{s_y}} \quad (9)$$

In addition, the concrete average tensile stress ( $f_{c1}$ ) should be limited by the reserve capacity of the reinforcement. In the solution procedure of the MCFT, this limit is checked using a relationship between  $v_{cimax}$  and  $f_{c1}$  derived by substituting Eq. (7) into the local equilibrium equations (Eq. (4) and Eq. (5)). For instance, assuming the reinforcement in the Y direction is the weaker reinforcement, then the following condition should be satisfied:

$$f_{c1} \leq v_{c\max}[0.18 + 0.3(1.64 - \cot \theta_c)^2] \tan \theta_c + \rho_{sy}(f_{yy} - f_{sy}) \quad (10)$$

### Compatibility Relations

Since perfect bond is assumed between the concrete and reinforcement, compatibility conditions require that the deformation of the concrete and reinforcement be identical. Therefore, the average strain in the reinforcement should be equal to that in the concrete in the corresponding direction:

$$\varepsilon_x = \varepsilon_{cx} = \varepsilon_{sx} \quad ; \quad \varepsilon_y = \varepsilon_{cy} = \varepsilon_{sy} \quad (11)$$

where  $\varepsilon_x$  and  $\varepsilon_y$  are the element total strains,  $\varepsilon_{cx}$  and  $\varepsilon_{cy}$  are the concrete total strains, and  $\varepsilon_{sx}$  and  $\varepsilon_{sy}$  are the reinforcement total strains in the X and Y directions. If the total strains in the X and Y directions are known, with the aid of a Mohr's circle, the total strains in the principal directions ( $\varepsilon_{c1}$ ,  $\varepsilon_{c2}$ ) and the crack inclination ( $\theta_c$ ) can be found:

$$\varepsilon_{c1}, \varepsilon_{c2} = \frac{(\varepsilon_{cx} + \varepsilon_{cy})}{2} \pm \frac{1}{2} \sqrt{(\varepsilon_{cx} - \varepsilon_{cy})^2 + \gamma_{cxy}^2} \quad (12)$$

$$\theta_c = \frac{1}{2} \tan^{-1} \left[ \frac{\gamma_{cxy}}{\varepsilon_{cy} - \varepsilon_{cx}} \right] \quad (13)$$

It must be remembered that the inclinations of the principal strains and principal stresses are assumed equal in the MCFT formulation.

### Constitutive Relations

**Stress-strain relations for concrete** — the compressive response of concrete is shown in **Fig. 1(o)**. The compression softening effect is taken into account by representing the principal compressive stress ( $f_{c2}$ ) as a function of both the principal compressive strain ( $\varepsilon_{c2}$ ) and the principal tensile strain ( $\varepsilon_{c1}$ ):

$$f_{c2} = f_{c2\max} \left[ 2 \left( \frac{\varepsilon_{c2}}{\varepsilon'_c} \right) - \left( \frac{\varepsilon_{c2}}{\varepsilon'_c} \right)^2 \right] \quad (14)$$

$$f_{c2\max} = \frac{f'_c}{0.8 - 0.34 \left( \frac{\varepsilon_{c1}}{\varepsilon'_c} \right)} \leq f'_c \quad (15)$$

where  $f'_c$  and  $\varepsilon'_c$  are the concrete cylinder compressive strength and the corresponding strain.

The tensile response of concrete is shown in **Fig. 1(n)**. Prior to cracking, the response is assumed to be linear:

$$f_{c1} = E_c \times \varepsilon_{c1} \quad (\varepsilon_{c1} \leq \varepsilon_{cr}) \quad (16)$$

where  $E_c$  is the concrete elastic modulus and  $\varepsilon_{cr}$  is the concrete cracking strain.

After cracking, experimental results showed that even at large tensile strain values, significant levels of tensile stress were carried by the concrete between the crack locations. This observation led to the development of a preliminary tension stiffening relationship:

$$f_{c1} = \frac{f_{cr}}{1 + \sqrt{200\varepsilon_{c1}}} \quad (\varepsilon_{c1} \geq \varepsilon_{cr}) \quad (17)$$

where  $f_{cr}$  is the concrete cracking stress. Collins et al. (1996) suggested that for larger elements using “500” instead of the “200” in the denominator is more suitable.

**Stress-strain relations for reinforcement** — the reinforcement response in compression and tension is represented by a bilinear relationship (see **Fig. 1(q)**):

$$f_{sx} = E_{sx} \times \varepsilon_{sx} \leq f_{yx} \quad (18)$$

$$f_{sy} = E_{sy} \times \varepsilon_{sy} \leq f_{yy} \quad (19)$$

where  $E_{sx}$  and  $E_{sy}$  are the elastic modulus of the reinforcement in the reference directions.

## APPLICATION TO BEAMS

Vecchio and Collins (1988) developed an iterative procedure based on the MCFT for analysis of reinforced concrete beams. In this procedure, the cross section is divided into a number of concrete layers and longitudinal reinforcing bar layers. Each layer is defined based on its geometry and material properties. The procedure assumes “plane sections remain plane” which allows the calculation of the longitudinal strain throughout the cross section as follows:

$$\varepsilon_{xi} = \varepsilon_t - \frac{(\varepsilon_b + \varepsilon_t)}{h} y_i \quad (20)$$

where  $\varepsilon_{xi}$  is the longitudinal strain of the  $i^{\text{th}}$  layer,  $\varepsilon_t$  and  $\varepsilon_b$  are the strains of the top and bottom layers,  $y_i$  is the distance from top of the section to the  $i^{\text{th}}$  layer, and  $h$  is the section height.

Two types of methods were proposed to determine the shear stress distribution: 1) a rigorous method in which the shear stresses are calculated from the analysis of two sections of the beam located close to each other, and 2) approximate methods based on a uniform shear stress distribution or a parabolic shear strain distribution assumption.

Fig. 4 shows the layered beam model with the linear longitudinal strain distribution and the parabolic shear strain distribution.

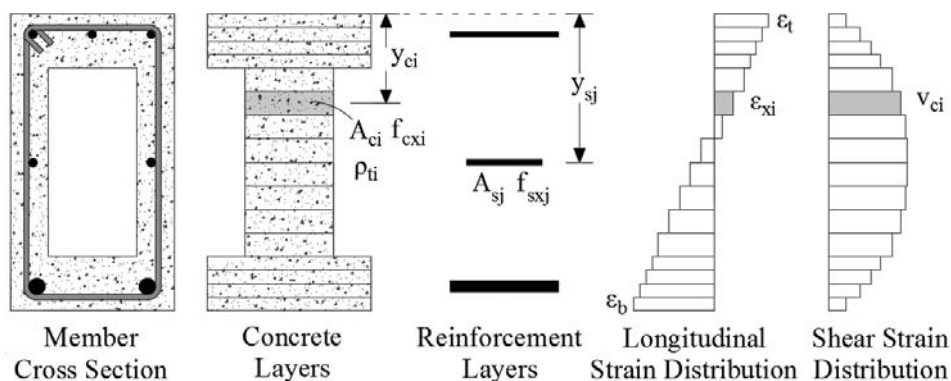


Figure 4 — Longitudinal and shear strain distributions in layered beam model

Knowing the longitudinal strain and shear stress distributions, and with the aid of the MCFT formulation, the longitudinal stresses for the concrete layers ( $f_{cx}$ ) and the reinforcement layers ( $f_{sx}$ ) can be determined. To satisfy equilibrium requirements, the resultant forces from the internal stresses must equal to the applied sectional forces. Therefore:

$$N = \sum_{i=1}^m f_{cxi} A_{ci} + \sum_{j=1}^n f_{sxj} A_{sj} \quad (21)$$

$$M = \sum_{i=1}^m f_{cxi} A_{ci} (y_{ci} - \bar{y}) + \sum_{j=1}^n f_{sxj} A_{sj} (y_{sj} - \bar{y}) \quad (22)$$

$$V = \sum_{i=1}^m v_{ci} A_{ci} \quad (23)$$

where  $N$ ,  $M$ , and  $V$  are the applied axial, moment, and shear loads, respectively,  $A_{ci}$  and  $y_{ci}$  are the area and distance of the  $i^{\text{th}}$  concrete layer from the top of the section,  $A_{sj}$  and  $y_{sj}$  are the area and distance of the  $j^{\text{th}}$  reinforcement layer with respect to the top of the section, and  $\bar{y}$  is the distance of the neutral axis from the top of the section. The equilibrium equations assume zero clamping stresses ( $f_y = 0$ ) and no dowel action from the reinforcement. The procedure is formulated in an iterative manner in which the longitudinal strain distribution is adjusted so that the equilibrium conditions are satisfied. Vecchio and Collins (1988) verified the method through analysis of different series of beam specimens reported in the literature. Bentz (2000) improved the procedure by introducing a rigorous longitudinal stiffness method to more accurately calculate the nonlinear shear stress distribution through the cross section. The procedure was implemented into Response-2000 (Bentz, 2000), a nonlinear sectional analysis program for reinforced concrete members. In recent years, Guner and Vecchio (2010; 2012) extended the application of the method to the analysis of reinforced concrete frames under static and dynamic loads, and developed the VecTor5 program, a nonlinear sectional analysis software for two-dimensional frame structures based on the MCFT and DSFM.

## ADAPTATION TO FINITE ELEMENT ANALYSIS

### Generalized Formulation

The MCFT formulation can be generalized to include any number of reinforcement components in arbitrary directions. With this type of formulation, the local stress in the reinforcement can be determined from the equilibrium equation in the direction normal to the crack surface:

$$f_{c1} = \sum_{i=1}^n \rho_i \times (f_{scri} - f_{si}) \cos^2(\Theta - \alpha_i) \quad (24)$$

where  $\rho_i$ ,  $f_{scri}$ ,  $f_{si}$ , and  $\alpha_i$  are the reinforcement ratio, the local reinforcement stress, the average reinforcement stress, and the inclination of the  $i^{\text{th}}$  reinforcement component, respectively, and  $\Theta$  is the inclination of the principal tensile stress. It should be noted that the original MCFT formulation was defined based on the crack orientation ( $\Theta_c$ ), while the generalized MCFT and the DSFM model formulations are represented based on the inclination of the principal tensile stress ( $\Theta$ ) which is perpendicular to  $\Theta_c$  (see Fig. 5).

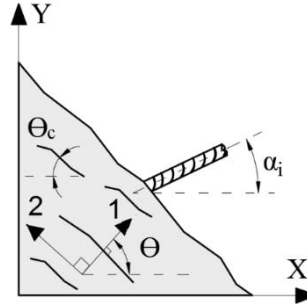


Figure 5 — Inclination of principal tensile stress and  $i^{\text{th}}$  reinforcement component

From the compatibility conditions at the crack surface, the local strain of the  $i^{\text{th}}$  reinforcement component ( $\varepsilon_{\text{scri}}$ ) can be determined using the average reinforcement strain ( $\varepsilon_{\text{si}}$ ) and the local incremental strain ( $\Delta\varepsilon_{\text{cri}}$ ).

$$\varepsilon_{\text{scri}} = \varepsilon_{\text{si}} + \Delta\varepsilon_{\text{cri}} \times \cos^2(\theta - \alpha_i) \quad (25)$$

The local incremental strains are computed such that the resultant local reinforcement stresses satisfy the equilibrium equation expressed in Eq. (24). Also, the requirement for the principal tensile stress can be written as:

$$f_{c1} \leq \sum_{i=1}^n \rho_i \times (f_{yi} - f_{si}) \cos^2(\theta - \alpha_i) \quad (26)$$

where  $f_{yi}$  is the yield strength of the  $i^{\text{th}}$  reinforcement component. Using the equilibrium equation in the direction perpendicular to the crack surface, the interface shear stress can be determined:

$$v_{ci} = \sum_{i=1}^n \rho_i \times (f_{\text{scri}} - f_{si}) \cos(\theta - \alpha_i) \sin(\theta - \alpha_i) \quad (27)$$

### Matrix Formulation

Vecchio (1989) presented the MCFT in a matrix form to facilitate implementation of the model into the finite element analysis programs. For this type of formulation, the 2D stress-strain relationship of an RC element can be written as:

$$\begin{Bmatrix} \sigma_x \\ \sigma_y \\ \tau_{xy} \end{Bmatrix} = \begin{bmatrix} D_{11} & D_{12} & D_{13} \\ D_{21} & D_{22} & D_{23} \\ D_{31} & D_{32} & D_{33} \end{bmatrix} \times \begin{Bmatrix} \varepsilon_x \\ \varepsilon_y \\ \gamma_{xy} \end{Bmatrix} - \begin{Bmatrix} \sigma_x^0 \\ \sigma_y^0 \\ \tau_{xy}^0 \end{Bmatrix} \quad (28)$$

where  $\{\sigma\}$  and  $\{\varepsilon\}$  are the total stress and strain vectors,  $[D]$  is the composite material stiffness matrix, and  $\{\sigma^0\}$  is the pseudo-stress vector which was later introduced by Vecchio (1992) to account for elastic and plastic strain offsets.

The composite material stiffness matrix,  $[D]$ , can be constructed by superposition of the material stiffness matrices of the concrete and all reinforcement components, with respect to an arbitrary X,Y reference system, as follows:

$$[D] = [T_c]^T [D_c]' [T_c] + \sum_{i=1}^n [T_s]_i^T [D_s]'_i [T_s]_i \quad (29)$$

The concrete material stiffness matrix,  $[D_c]'$ , is calculated using the effective secant moduli of concrete ( $\bar{E}_{c1}$ ,  $\bar{E}_{c2}$ ,  $\bar{G}_c$ ) defined with respect to the principal directions as follows:

$$[D_c]' = \begin{bmatrix} \bar{E}_{c1} & 0 & 0 \\ 0 & \bar{E}_{c2} & 0 \\ 0 & 0 & \bar{G}_c \end{bmatrix} \quad (30)$$

$$\bar{E}_{c1} = \frac{f_{c1}}{\varepsilon_{c1}} ; \bar{E}_{c2} = \frac{f_{c2}}{\varepsilon_{c2}} ; \bar{G}_c = \frac{\bar{E}_{c1} \times \bar{E}_{c2}}{\bar{E}_{c1} + \bar{E}_{c2}} \quad (31)$$

The material stiffness matrix of the  $i^{\text{th}}$  reinforcement component,  $[D_s]'$ , is determined using the effective secant modulus of steel ( $\bar{E}_{si}$ ) defined in the direction of the reinforcing bar as follows:

$$[D_s]'_i = \begin{bmatrix} \rho_{si} \bar{E}_{si} & 0 & 0 \\ 0 & 0 & 0 \\ 0 & 0 & 0 \end{bmatrix} \quad (32)$$

$$\bar{E}_{si} = \frac{f_{si}}{\varepsilon_{si}} \quad (33)$$

In Eq. (29),  $[T_c]$  and  $[T_s]_i$  are the transformation matrices for the concrete and  $i^{\text{th}}$  reinforcement component to convert the material stiffness matrices to the reference X and Y directions.

In a finite element analysis program, the element stiffness matrix,  $[k]$ , can be determined from the matrix  $[D]$ :

$$[k] = \int_{Vol} [B]^T [D] [B] dV \quad (34)$$

where  $[B]$  is the strain function matrix derived from the element shape functions. Assembling the stiffness matrix of all the elements results in the structure stiffness matrix,  $[K]$ , which can be used to calculate the nodal displacement vector,  $\{u\}$ , as follows:

$$\{u\} = [K]^{-1}\{p\} \quad (35)$$

where  $\{p\}$  is the nodal force vector. From the nodal displacement vector, new sets of strains and stresses in each element can be calculated. This procedure is repeated until the calculated values are converged and final results are obtained.

### **VecTor Suite of Programs**

The MCFT has served as the material modeling basis for several finite element and sectional analysis software. One of the most comprehensive analytical tools developed based on the model is the VecTor suite of programs, a set of six nonlinear finite element analysis software each specialized for a particular type of structure. These programs are VecTor2 (applicable to two-dimensional RC membrane structures) (Wong and Vecchio, 2002; Wong et al., 2013), VecTor3 (applicable to three-dimensional RC solid structures) (Vecchio and Selby, 1991; ElMohandes and Vecchio, 2013), VecTor4 (applicable to three-dimensional RC shell and plates) (Polak and Vecchio, 1993; Hrynyk and Vecchio, 2010), VecTor5 (applicable to two-dimensional RC frames) (Guner and Vecchio, 2010), and VecTor6 (applicable to three-dimensional axisymmetrical solid structures) (Montoya, 2003; Lulec, 2017). Over the last three decades, the improvements in the MCFT and extension of its formulation to more advanced research areas have been implemented in VecTor, greatly increasing the programs' capabilities.

### **DISTURBED STRESS FIELD MODEL (DSFM)**

In most verification tests, the MCFT has been able to capture the experimental responses with high accuracy (Vecchio et al., 2001); however, some deficiencies regarding specific situations have been noted (Vecchio, 2000). For panels with high amounts of reinforcement or panels subjected to shear and biaxial compression, where there was little or no rotation in the crack direction, the MCFT typically underestimated the shear strength and stiffness. For panels with low amounts of reinforcement that exhibited significant rotation in the crack direction and slippage along the crack surface, the MCFT had a tendency to overestimate the shear strength and stiffness. Examination of the test data revealed that the reduced accuracy in these situations was mainly due to two simplifying assumptions used in the model: 1) the orientations of the average principal stresses and the average principal strains remain coincident throughout the test, and 2) neglecting the shear slip deformations along the crack surface. The Disturbed Stress Field Model (DSFM) (Vecchio, 2000) is an extension of the MCFT that takes into account the crack slip deformations in the compatibility relations, allowing for the deviation of the principal stress field from the principal strain field. The refinements of the DSFM compared to the original formulation are summarized in the following subsections.

#### **Equilibrium Relations**

The DSFM equilibrium relations are similar to the generalized MCFT formulation, as presented in Eq. (24) to Eq. (27), applicable to elements with any number of reinforcement components. Unlike the MCFT, the DSFM does not require the shear stress check on the crack surface (Eq. (6)) since the shear slip deformations are taken into account in the compatibility relations. **Fig. 6** shows the stress conditions at the crack locations and between the cracks according to the DSFM model.

#### **Compatibility Relations**

Results from panel element tests showed that, in general, the change in the orientation of the average concrete principal stresses is less than that observed for the average concrete principal strains. The principal strain orientation is affected by both the continuum strains (i.e., net strains) caused by applied stresses and the discontinuous slip deformations along the crack surface, while the principal stresses orientation is only influenced by the continuum strains. The DSFM decouples the total strains ( $\epsilon_x, \epsilon_y, \gamma_{xy}$ ) in the element into the concrete net strains ( $\epsilon_{cx}, \epsilon_{cy}, \gamma_{cxy}$ ) and the concrete crack slip strains ( $\epsilon_x^s, \epsilon_y^s, \gamma_{xy}^s$ ):

$$\epsilon_x = \epsilon_{cx} + \epsilon_x^s \quad ; \quad \epsilon_y = \epsilon_{cy} + \epsilon_y^s \quad ; \quad \gamma_{xy} = \gamma_{cxy} + \gamma_{xy}^s \quad (36)$$

Using a Mohr's circle for each set of strains, the corresponding principal strains and their orientation can be determined. It can be seen that the orientation of the concrete net principal strains ( $\Theta$ ) is similar to the orientation of the concrete principal stresses ( $\Theta_\sigma$ ) and is different than the orientation of the total principal strains ( $\Theta_\epsilon$ ).

To compute the concrete crack slip strains, an average shear slip strain ( $\gamma_s$ ) is defined as the following:

$$\gamma_s = \frac{\delta_s}{s} \quad (37)$$

where  $s$  is the average crack spacing as defined in the MCFT and  $\delta_s$  is the slip along the crack surface determined based on a slip model. The default slip model currently used is the one proposed by Walraven (1981) as follows:

$$\delta_s = \frac{v_{ci}}{1.8w^{-0.8} + (0.234w^{-0.707} - 0.20)f_{cc}} \quad (38)$$

where  $f_{cc}$  is the concrete compressive cube strength,  $v_{ci}$  is the shear stress along the crack surface determined from Eq. (27), and  $w$  is the average crack width estimated from Eq. (8).

Constructing a Mohr's circle for the average shear slip strain ( $\gamma_s$ ), yields the following relations for the strain components relative to the X and Y directions:

$$\epsilon_x^s = -\frac{\gamma_s}{2} \sin 2\theta \quad ; \quad \epsilon_y^s = \frac{\gamma_s}{2} \sin 2\theta \quad ; \quad \gamma_{xy}^s = \gamma_s \cos 2\theta \quad (39)$$

Fig. 7 shows the average deformations, local deformations due to slip along the crack surface, and total deformations of an RC element.

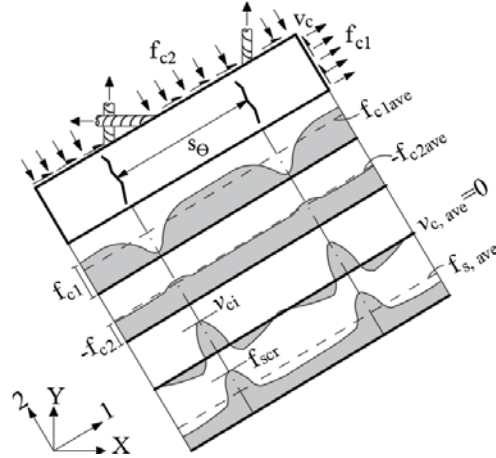


Figure 6 — Stress conditions at crack locations and between cracks

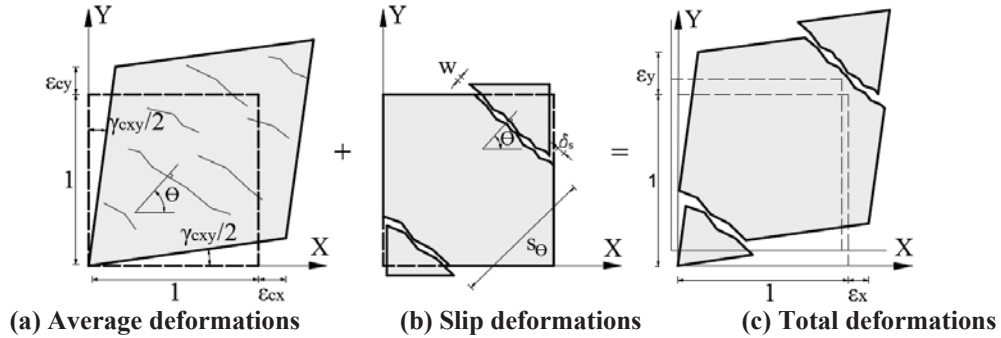


Figure 7 — DSFM compatibility conditions

Because of the assumption of perfect bond between the concrete and reinforcement, the average strain in the reinforcement should be computed from the total strains. At the crack surface, the local stresses and strains in the reinforcement are calculated using a similar procedure to that described for the MCFT in Eq. (24) and Eq. (25).

**Constitutive Relations**

**Stress-strain relations for concrete** — to consider the compression softening response of concrete, a reduction factor ( $\beta_d$ ) was introduced as the following:

$$\beta_d = \frac{1}{1 + C_s C_d} \leq 1.0 \quad (40)$$

The  $C_d$  factor is a function of the principal compressive strain ( $\epsilon_{c2}$ ) and the coexisting principal tensile strain ( $\epsilon_{c1}$ ). Further analysis of the data obtained from panel element tests revealed that considering the crack slip deformations in the compatibility relations results in a more softened element response, but less softened concrete response, relative to the MCFT; therefore, the rate of the strength degradation due to the transverse cracking must be reduced. This reduction is taken into account by the  $C_s$  factor. Using  $C_s = 0.55$  produced the best fit to the test data when applying the DSFM;  $C_s = 1.0$  is implied when using the MCFT.

The  $\beta_d$  factor is used to reduce both the peak strength ( $f_p$ ) and the corresponding strain ( $\epsilon_p$ ) in the concrete compressive stress-strain relationship as follows (see **Fig. 1(t)**):

$$f_p = \beta_d f'_c \quad ; \quad \epsilon_p = \beta_d \epsilon'_c \quad (41)$$

Similar to the MCFT, the tensile response of concrete before cracking is considered using a linear relation presented in Eq. (16). After cracking, the DSFM considers two independent mechanisms (tension softening and tension stiffening) to determine the residual concrete tensile stress. The post-cracking tensile stress resulting from the tension softening mechanism ( $f_{c1}^a$ ) is determined using a fracture mechanics relation as follows:

$$f_{c1}^a = f_{cr} \left[ 1 - \frac{(\epsilon_{c1} - \epsilon_{cr})}{(\epsilon_{ts} - \epsilon_{cr})} \right] \quad (42)$$

where  $\epsilon_{ts}$  is the terminal strain calculated from the concrete fracture energy. The tension softening mechanism is particularly significant in lightly reinforced concrete members.

The post-cracking tensile stress produced from the tension stiffening mechanism ( $f_{c1}^b$ ) is calculated based on a model proposed by Bentz (2000) which was later modified by Vecchio (2000) to account for reinforcement with arbitrary directions:

$$f_{c1}^b = \frac{f_{cr}}{1 + \sqrt{c_t \epsilon_{c1}}} \quad (43)$$

The MCFT uses a constant number for the  $c_t$  factor (200 for small elements and 500 for large elements). Bentz (2000) showed that the tension stiffening is also a function of the reinforcement ratio ( $\rho$ ) and the reinforcing bar diameter ( $d_b$ ), and defined the  $c_t$  factor accordingly.

**Fig. 1(r)** and **Fig. 1(s)** show the tension softening and the tension stiffening mechanisms in the DSFM, respectively. The average principal tensile stress ( $f_{c1}$ ) is defined as the larger of the two mechanisms:

$$f_{c1} = \max(f_{c1}^a, f_{c1}^b) \quad (44)$$

**Stress-strain relations for reinforcement** — the DSFM uses a stress-strain relationship for the reinforcement similar to that of the MCFT except it considers strain hardening effects. Prior to strain hardening, the response can be expressed using the relationship in Eq. (18). After the strain hardening, the following equation is used to determine the response of the  $i^{\text{th}}$  reinforcement component in both tension and compression:

$$f_{si} = f_{yi} + E_{shi}(\epsilon_{si} - \epsilon_{shi}) \quad (\epsilon_{shi} < \epsilon_{si} < \epsilon_{ui}) \quad (45)$$

where  $E_{shi}$  is the strain hardening modulus,  $\epsilon_{shi}$  is the strain hardening strain, and  $\epsilon_{ui}$  is the ultimate strain. The reinforcement response is shown in **Fig. 1(u)**.

## VERIFICATION STUDIES

Over the last several years, the accuracy of the MCFT and DSFM models have been examined through the analyses of various types of test specimens (e.g., Vecchio et al., 2001; Palermo and Vecchio, 2007; Hunter 2016) as well as real-world structures (e.g., Vecchio, 2002; Vecchio et al., 2004). In this section, summaries of three comprehensive verification studies that were performed on panel element, shear wall, and beam specimens using the VecTor2 program are presented as examples.

### Verification against Panel Element Tests

Vecchio et al. (2001) modeled three series of panel element specimens, a total of 40 specimens, using both the MCFT and DSFM models and compared the analytical results against the experimental behavior. The specimens varied in terms of the concrete compressive strength, the longitudinal and transverse reinforcement ratios, and the loading condition. In general, the analytical and experimental load-deflection responses agreed reasonably well. With the MCFT model, the computed shear strength had a mean analytical to experimental value of 1.05 with a coefficient of variation (COV) of 10.3%. With the DSFM model, the load-deflection responses were estimated more accurately than the MCFT, and resulted in a mean analytical to experimental value of 1.02 with a COV of 9.6% for the shear strength. The study also concluded that the analytical responses for uniaxially reinforced panels were highly sensitive to the concrete cracking strength. Since this is an extremely variable parameter, regardless of the analysis procedure, modeling of such members with a high level of accuracy may not be consistently achieved.

### Verification against Shear Wall Tests

Palermo and Vecchio (2007) examined the accuracy of the DSFM model by performing a parametric study on 21 large-scale shear walls ranging from slender to squat with various types of cross sections tested under reversed cyclic loading conditions. The analytical procedure fairly accurately captured the experimental behavior in terms of the peak load capacity, ductility, energy dissipation, and failure mode. The ratio of the computed-to-observed shear strength obtained using VecTor2 had a mean of 1.01 and a COV of 6.1%; for the lateral displacement at ultimate strength, the corresponding numbers were 1.09 and 36.4%. Clearly, accurately calculating deformation capacity consistently remains a challenge. Vecchio et al. (2001) conducted a similar analytical study on two series of large-scale shear walls,

a total of 13 specimens, tested under monotonic loading conditions. The specimens varied in terms of the level of axial load, height-to-width ratio, and amount of reinforcement. The results computed by the MCFT and DSFM models were almost identical. The ratio of the calculated-to-measured strength for all the shear walls had a mean of 1.01 with a COV of 5.3%. The computed failure mode consisted of concrete crushing in the toe region combined with a sliding shear failure along the base, agreeing well with the experimentally observed behavior. Overall, the ductility of the shear walls was computed with reasonable accuracy as well.

**Verification against Beam Tests**

Hunter (2016) assessed the professional factor (a random variable that captures the uncertainty of a numerical model) of the VecTor2 program for analysis of shear-critical beams with no transverse reinforcement. The study included modeling a total of 376 shear-critical beams, which had sufficient testing information, selected from a database reported by Reineck et al. (2013). The beams had a rectangular cross section with span-to-depth ratios greater than 2.41, and were subjected to a one-point or two-point bending test. Based on the analysis results, the professional factor, defined as the ratio of the calculated-to-measured peak load, had a mean of 0.94 and a COV of 18.7%. Similar analyses were performed with the CSA A23.3 and ACI-318 design codes. The CSA A23.3 code whose shear design provisions are based on a simplified version of the MCFT resulted in acceptable and safe predications for the shear strength of the majority of the beams. However, the results obtained from the ACI-318 code were highly conservative for beams with effective depths less than 500 mm and, more importantly, were unconservative for beams with effective depths greater than 750 mm. This was mainly attributed to neglecting the size effect in the shear design provisions of the ACI-318 code. Another parametric study on the behavior of shear-critical beams was undertaken by Vecchio (2001). In this study, three series of beams with little or no transverse reinforcement (a total of 54 specimens) were modeled with the MCFT and DSFM. The ratio of the calculated-to-observed shear capacity obtained from the MCFT had a mean of 1.00 with a COV 20.3%. The DSFM resulted in improved analytical responses with the mean of 1.07 and COV of 16.9%. For shear-critical beams containing no shear reinforcement, these should be considered good results.

Fig. 8 shows the calculated-to-measured load capacity for all the specimens of the aforementioned verification studies.

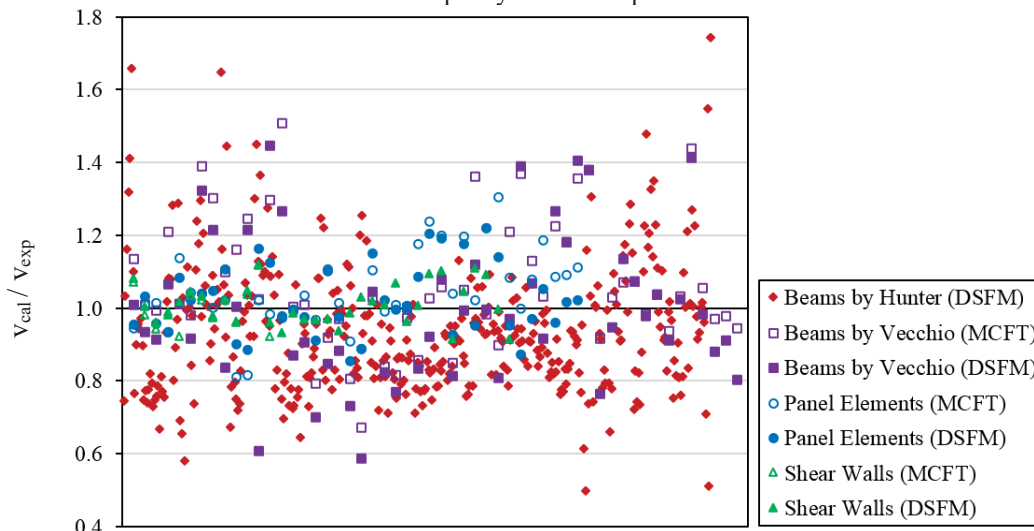


Figure 8 — Calculated-to-measured load capacity for MCFT and DSFM

**RECENT ADVANCES**

In recent years, the application of the MCFT has been extended to more advanced research areas. In addition, pre- and post-processors have been developed for the VecTor suite of software contributing to the programs’ utility. A summary of these advancements and the related references are presented in the following.

**Pre- and Post-Processors**

A generalized user-friendly pre-processor, FormWorks-Plus (Sadeghian and Vecchio, 2015), has been developed to facilitate the process of creating finite element models for the VecTor suite of programs. FormWorks-Plus is an extended version of FormWorks (Wong and Vecchio, 2002) which was a graphical user-interface specialized for the VecTor2 program. The pre-processors provide easy-to-use features for the user to create the finite element mesh and define materials, loads, and support conditions. They also perform a series of checks to ensure the finite element model is defined properly and in accordance with the format required for the VecTor programs inputs. FormWorks is enhanced with a two-dimensional auto-meshing feature, facilitating the mesh generation process. FormWorks-Plus,

which is compatible with all the VecTor programs, provides a wide range of viewing options, enabling modeling structures with complex geometries.

Most academic analysis software, including the VecTor programs, store the analysis results in a series of text files. However due to the substantial volume of output data, accessing the relevant analysis information is often a time-consuming and error-prone process. A graphical post-processor, named Janus (Chak, 2013), has been developed that allows the user to comprehensively recall and manipulate structural analysis results both at the system-level and element-level. Janus is capable of displaying different response characteristics of the structure including deformed shape, stress and strain variations in the concrete and reinforcing bar elements, and various types of graphs. The program has been recently improved to display the crack propagation and the element sectional view for frame structures (Loya et al., 2017). Janus is compatible with all the VecTor programs. For VecTor2, the post-processor program Augustus (Bentz, 2000) is the preeminent tool for visualization of the analysis results.

#### **Application to Advanced Loading Conditions**

**Dynamic analysis** — in recent years, with elevated terror threats around the world, the need for accurate analysis of RC structures subjected to blast and impact loads has been significantly increased. Test results have shown that RC structures typically experience a shear-dominant behavior under impact loads. The MCFT, which was successfully employed for the analysis of shear-critical members under static loads, was further extended to consider dynamic loads (Saatci and Vecchio, 2009). For this purpose, the original tangent-stiffness-based formulation of Newmark's method (Newmark, 1959) was presented in the form of total-load secant-stiffness formulation similar to that used in the MCFT. The procedure was implemented in VecTor2 and verified through the analysis of a series of beam specimens subjected to impact loads. The analytical and experimental results agreed well in terms of the failure modes, displacements, and damage levels. The minor discrepancies were attributed to deficiencies regarding modeling the strain rate effects. Guner and Vecchio (2012) derived a simplified version of the method for sectional analysis of RC frames under dynamic loads. They incorporated proper concrete and reinforcement strain rate models into the dynamic formulation of the MCFT, improving the accuracy of the method. Trommels (2013) performed a numerical study to assess the analysis capabilities of VecTor2 and VecTor3 for impact and impulse loading conditions. The study demonstrated the importance of proper modeling of the support conditions and the shape of the pressure-time profile. Hrynyk (2013) extended the method to three-dimensional analysis of reinforced concrete and fiber-reinforced concrete shells subjected to high-mass low-velocity impact loads. Lulec (2017) further developed the method for analysis of three-dimensional and axisymmetric RC solid structures under blast and hard missile impact loading conditions. Missile perforation velocities were estimated using a semi-analytical relationship based on the MCFT. A series of verification tests was performed to examine the accuracy of the analytical procedure. Overall, the analytical and experimental results were in good agreement in terms of the time-displacement response and damage mode.

**Fire analysis** — advanced modeling of RC structures subjected to fire has been the focus of researchers for many decades. However, current analytical tools typically have major deficiencies in considering simultaneously both thermal- and structural-related mechanisms. More importantly, they are typically unable to accurately compute the shear behavior of RC structures under elevated temperatures. ElMohandes and Vecchio (2016) proposed a time stepping procedure, developed based on the MCFT, which considers the thermal- and structural-related mechanisms in a coupled manner. The procedure consists of two levels of analysis. At the first level, a nonlinear heat transfer analysis is performed at certain time steps to determine the thermal expansion strains and reduction factors for the temperature-dependent mechanical properties of the concrete and reinforcement. The heat transfer analysis can be paired with a moisture transfer analysis that enables calculating the additional tensile stresses resulted from the vapor pressure developed in the concrete pores. At the second level, a nonlinear structural analysis is performed taking into account the first level analysis results as well as the externally applied loads. The proposed procedure was implemented in VecTor3 and was successfully verified through coupled thermal and structural analysis of a series of RC column specimens reported in the literature.

**Fatigue analysis** — recently, Isojeh et al. (2017a; 2017b; and 2017c) experimentally investigated the behavior of reinforced concrete and steel-fiber concrete elements subjected to fatigue loading and proposed a set of damage and constitutive models for the concrete composites (including steel fibers) and a crack-growth model for the reinforcement. These models were incorporated into the DSFM formulation enabling analysis of concrete structures under a fatigue loading condition. With this analysis procedure, first a set of material damage values for a certain number of fatigue loading cycles is evaluated. Then, the structure is analyzed under the externally applied loads taking into account the fatigue damage effects. The analytical procedure was corroborated by examining the behavior of a series of small-scale reinforced concrete and steel-fiber concrete deep beams tested under fatigue loads. In general, the analytical load-deflection responses agreed well with the experimentally observed behavior.

### **Application to Other Materials**

**Steel fiber-reinforced concrete (SFRC)** — the addition of steel fibers to concrete has been shown to considerably improve the post-cracking tensile strength, shear resistance, and crack control characteristics of the material. Susetyo et al. (2013) assessed the performance of then current concrete constitutive models in computing the behavior of SFRC panel specimens subjected to pure shear, and found that the analysis results overestimated the strength and deformation capacity of the SFRC panels. It was concluded that the accuracy of the analysis was greatly dependent on the tension stiffening and softening models, the consideration of shear slip on the crack surface, and the crack spacing parameter. Lee et al. (2016) modified the MCFT and DSFM formulations and proposed a new method for analysis of SFRC members. To accurately consider second-order material effects, the method uses constitutive relationships specifically derived for the SFRC material. The contribution of steel fibers to the post-cracking tensile strength is considered with the Diverse Embedment Model (DEM) (Lee et al., 2011) or the simpler SDEM (Lee et al., 2013a). The more rigorous DEM uses a double numerical integration scheme to evaluate the fiber tensile stress at the crack location. The SDEM, which is a simplified version of the DEM, evaluates the influence of the pullout mechanism and the end anchorage on the bond behavior separately using simple equations. For SFRC members containing conventional reinforcement, the tension stiffening model used in the DSFM was modified to include the influence of steel fibers (Lee et al., 2013b). The shear stress at the crack surface and the upper limit of the concrete post-cracking tensile stress are calculated similar to the MCFT with the addition of a new term representing the contribution of steel fibers bridging the crack surface. In the analytical procedure, both the shear slip and the fiber tensile stress relationships are presented as a function of the crack width which can be determined using a SFRC crack spacing model developed by Deluce et al. (2014). Lee et al. (2016) successfully verified the procedure through analysis of a series of SFRC panels tested under shear.

**Steel-concrete composite** — steel-concrete (SC) composite elements generally consist of a thick concrete core attached to two thin steel faceplates with regularly spaced stud anchors. Common micro-modeling methods for analysis of such elements require detailed three-dimensional modeling of every component including the individual anchor studs, making their applications to large structures questionable. Vecchio and McQuade (2011) adopted the DSFM formulation and proposed a macro-modeling approach which facilitates analysis of SC elements. With this method, similar to the concrete and reinforcement formulations, the total strains in the steel plates are expressed as a summation of the offset and net strains. The material stiffness matrix for the steel plates is defined as a diagonal matrix using appropriate secant moduli. The von Mises criterion is used to take into account the yielding of the steel plates under biaxial stress conditions. A number of simplifying assumptions have been made with respect to the interaction effects between the concrete and the steel plates; namely, the contribution from the steel plates to the concrete tension stiffening is neglected, maximum crack spacing is approximated as equal to the thickness of the SC element, and the interfacial slip between the concrete and the steel plates is neglected. In addition, the basic Euler buckling equation is used as an approximate method to consider the buckling of the steel plates. The performance of the method was assessed through analysis of SC panel elements and SC wall elements tested under monotonic and reversed cyclic loading conditions. In general, the analytical procedure was able to accurately compute the load-deflection responses and failure modes. There were some minor deficiencies which were attributed to the simplifying assumptions used in the procedure. Hrynyk and Vecchio (2016) extended the procedure to analysis of SC shell and plate structures and implemented the formulation into VecTor4. The performance of the method was successfully verified through the modeling of two series of SC specimens subjected to in-plane and out-of-plane loads reported in the literature.

**Alkali-silica reaction-affected concrete** — the deleterious effects of the alkali-silica reactive (ASR) aggregates on concrete behavior have been reported by several experimental studies and field observations. Ferche et al. (2017) modified the DSFM formulation and proposed a two-phase analysis approach to model the effects of ASR on reinforced concrete structures. In the first phase, the ASR expansion is evaluated in an iterative manner based on average long-term stress conditions using appropriate ASR models from the literature. Depending on the selected model, the ASR strains can be distributed uniformly in all directions or can have an anisotropic expansion along the principal directions. The ASR strains are incorporated into the DSFM formulation as elastic offset strains (for calculation of offset strains in the MCFT and DSFM refer to Vecchio (1992)). The ASR strains and their orientations remain constant through the remainder of the analysis. In addition, the degradation of concrete mechanical properties due to the ASR expansion can be either input manually, based on test results from sample specimens, or evaluated internally using the free expansion parameter. In the second phase, a nonlinear structural analysis is performed considering the results of the first phase and short-term loading conditions. The accuracy of the analytical procedure was evaluated through the modeling of three types of ASR-affected test specimens: cylinders, prisms, and RC beams. For all cases, the computed load-deflection responses agreed reasonably well with those obtained from the experiments. Recommendations were provided to further improve the results.

**Unreinforced masonry** — masonry is a composite orthotropic material comprised of blocks connected by mortar joints oriented in two perpendicular directions (i.e., head and bed joints). Facconi et al. (2014) developed a unique macro-modeling approach based on the DSFM for the analysis of unreinforced masonry structures. Unlike conventional smeared crack models, the proposed method is capable of considering the global behavior of the composite material in an average sense as well as the local shear slip response of the mortar joints. The equilibrium and compatibility relations are formulated similar to the DSFM. For the equilibrium equations, unlike with reinforced concrete, the shear stresses along the crack surface are assumed to be zero. For the compatibility equations, the total slip strain is calculated from the summation of the slip strains of the head and bed joints defined with respect to the X and Y directions. Also, the average crack spacing is defined as a function of the head and bed joint spacings. The compressive stress-strain relationship is represented with a concrete model modified according to the masonry characteristics. A failure criterion for masonry in compression, which takes into account the failures of the components and the composite material, is adopted. The masonry tensile response is assumed to be linear elastic prior to cracking and decay gradually after cracking (i.e., tension softening mechanism). The shear slip behavior of the masonry joints is represented with an elastic-plastic model based on the Mohr-Coulomb yield criterion. Details of the aforementioned models are provided by Facconi et al. (2014). The analytical procedure was verified against a full-scale masonry wall and building façade tests reported in the literature. The procedure was able to capture the experimental behavior for both ductile and brittle failure modes reasonably well.

#### **Application to RC Structures Repaired with FRP Sheets**

Fiber-reinforced polymer (FRP) composites have been shown to be an effective repair method to improve the performance of damaged RC structures. Various types of analytical models have been proposed to predict the behavior of RC structures repaired with FRP sheets. However, most of the studies have focused on the flexure-critical structures and the shear behavior of such structures has not been fully understood. Montoya et al. (2004) adopted the MCFT formulation and developed a constitutive relationship for concrete under the triaxial compression. The model was corroborated by analysis of several steel- and FRP-confined concrete column specimens. Sato and Vecchio (2003) developed a set of analytical models to represent the bond characteristics between the concrete and FRP sheets, and incorporated them into the DSFM formulation. The contributions of the FRP sheets to the crack formation and tension stiffening effects were formulated according to the equilibrium and compatibility conditions. A parametric study was performed to reduce the formulations into simplified models, enabling their implementation into the DSFM. The models were validated through analyses of a series of RC beam specimens containing externally bonded FRP sheets. Kim and Vecchio (2008) successfully employed the analytical procedure proposed by Sato and Vecchio (2003) for modeling a shear-critical RC frame repaired with FRP wrap. The bond between the concrete and the FRP wrap was modeled with two-noded non-dimensional link elements. The damage effects prior to repair were taken into account by recording the stress and strain history of the elements. Sadeghian and Vecchio (2016) extended the application of the method to multi-scale modeling, enabling analysis of large repaired RC structures. Details of the proposed multi-scale modeling approach is presented in the following sections.

#### **Application to Stochastic Analysis**

Stochastic simulation is often used to evaluate reliability indices for structural design codes. A reliability index defines the probability of structural failure in the limit state design method. Hunter (2016) implemented stochastic simulation techniques into VecTor2 for reliability analysis of shear-critical RC structures. Various types of statistic models for the concrete and reinforcement were adopted from the literature. The program was extended to perform Monte Carlo (MC) simulation, Latin Hypercube simulation (LHS), random field generation (both MC and LHS), and correlated sampling (both MC and LHS). Based on the selected stochastic simulation method, random samples are generated for the concrete and reinforcement material properties. The random sampled values are then used to modify the user defined material properties and generate random inputs for the analysis. By repeating the analysis with randomly generated inputs, the stochastic simulation derives probabilistic information regarding the structure. The application of the implemented stochastic simulation techniques was demonstrated by reliability analysis of shear-critical RC beams without transverse reinforcement for the CSA A23.3 (2014) and ACI-318 (2014) design codes. Habibi (2017) employed the stochastic tools of VecTor2 to investigate the sensitivity of the analysis results to the input parameters for corroded RC beam specimens. It was concluded that for RC beams damaged by uniform corrosion, modeling the rate of corrosion as a single variable rather than a random field results in more accurate statistical responses.

#### **Application to Multi-Platform Analysis and Hybrid Simulation**

Due to the complex behavior of cracked reinforced concrete, modeling an entire structure in fine detail using a nonlinear finite element analysis program may not be practical. In addition, situations often arise where a multi-disciplinary analysis may be warranted (e.g., soil-structure interaction analysis). Sadeghian (2017) developed a simulation framework, named Cyrus, for multi-platform analysis of RC structures. In this approach, based on the mechanical characteristics of the members and the anticipated locations of critical regions, the structural system is

divided into several substructures. Each substructure can be modeled using a wide range of analysis programs that are compatible with Cyrus including the VecTor suite of software. Cyrus coordinates the analysis and takes into account the interaction between the substructures. This allows a user to integrate different types of MCFT and DSFM formulations with each other (e.g., sectional analysis and finite element analysis) or with other types of analysis procedures available in structural software. The application of the proposed simulation framework was demonstrated through multi-platform analysis of several RC structures. In addition, a new interface element, named F2M element (Sadeghian et al., 2017a), was developed to connect layered beam elements to membrane elements in RC frames. The F2M element, which is based on the DSFM formulation, computes realistic stress distributions and allows for transverse expansion at the connection section between the two elements.

The simulation framework was further extended to combine numerical modules with experimental modules to accommodate hybrid testing (Sadeghian et al., 2017b). The physical modules are incorporated into the framework using a generalized controller interface program compatible with a wide range of laboratory equipment and testing configurations. The hybrid simulation capabilities of the framework were verified by conducting a small-scale experimental program using a six degrees-of-freedom hydraulic testing facility. The hybrid simulations included integration of the VecTor2 and VecTor5 programs with a small-scale test specimen.

### CONCLUSIONS

The MCFT, developed almost 40 years ago, remains an effective general model for analysis of reinforced concrete structures with detailed consideration of shear-related mechanisms. The MCFT shares the same principles as its predecessor model, CFT, as well as with its refined version, the DSFM. All three models are based on the smeared rotating crack concept, treat stresses and strains in an average sense, satisfy equilibrium and compatibility conditions, and represent cracked reinforced concrete as an orthotropic material with unique constitutive relationships. The models can be distinguished primarily in two aspects: 1) advancements in the constitutive relationships and 2) improvements in local considerations at the crack surface. Relative to the CFT, the MCFT takes into account the compression softening and tension stiffening mechanisms in the concrete constitutive relationships, and introduces the need to examine local stress conditions at crack locations. The DSFM incorporates further refinements in the constitutive models also takes into account shear slip along crack surfaces within the element compatibility formulations, thus allowing for the divergence of principal stress and principal strain directions.

Over the last three decades, the MCFT has been adapted to various types of sectional and finite element analysis programs as well as structural design codes. In addition, the formulations have been extended to several state-of-the-art research topics including extreme loading conditions, advanced material types, stochastic analysis, repaired structures, multi-scale analysis, and hybrid simulation. Many advancements were incorporated into the MCFT over the years; however, the fundamentals of the model remain unchanged.

The factors that make the MCFT a versatile and enduring model, which can be successfully applied to many diverse and complex structural problems with a high level of accuracy, can be summarized as follows:

- 1) The MCFT incorporates a rational and transparent approach based on simple and well-defined equations derived from fundamental principles of structural analysis and solid mechanics.
- 2) The nature of its formulation makes it easily adaptable to finite element analysis algorithms and other simple or advanced analysis procedures.
- 3) The MCFT provides a framework whereby a diverse range of constitutive models, behavior mechanisms, and material types can be included, enabling the consideration of a broad range of structures and loading conditions.
- 4) The MCFT does not rely on assumptions, material characterizations, or analysis calibrations that may vary from one type of structural element or load condition to another.
- 5) The smeared crack concept enables a macro-modeling approach, reducing modeling and computational effort.
- 6) Over the past four decades, the MCFT and its related analysis tools has benefitted from constant evolution and continuous verification using results from comprehensive well-defined testing programs.

### ACKNOWLEDGEMENT

The concept and preliminary formulation of the Modified Compression Field Theory were conceived by Professor Michael P. Collins, University of Toronto. The vision, guidance and encouragement he provided in its further development and application were essential to its success.

### REFERENCES

AASHTO LRFD Bridge Design Specifications 7<sup>th</sup> edition, American Association of State Highway and Transportation Officials, Washington, U.S.A., 2014, 2150 pp.

- ACI-ASCE Committee 445, "Recent Approaches to Shear Design of Structural Concrete," American Concrete Institute, 1999, 50 pp.
- ACI Committee 318, "Building Code Requirements for Reinforced Concrete and Commentary," American Concrete Institute, Detroit, U.S.A., 2014, 520 pp.
- ACI Committee 318, "Building Code Requirements for Reinforced Concrete," American Concrete Institute, Detroit, U.S.A., 1971, 78 pp.
- Bazant, Z. P., and Gambarova, P., "Crack Shear in Concrete: Crack Band Microplane Model," *ASCE Journal of Engineering Mechanics*, V. 110, 1984, pp. 2015-2035.
- Bentz, E. C., "Sectional Analysis of Reinforced Concrete Members," PhD Thesis, Department of Civil Engineering, University of Toronto, 2000, 310 pp.
- Bentz, E. C., Vecchio, F. J., and Collins, M. P., "The Simplified MCFT for Calculating the Shear Strength of Reinforced Concrete Elements," *ACI Structural Journal*, V.103, No. 4, 2006, pp. 614-624.
- Bhide, S., and Collins, M. P., "Influence of Axial Tension on the Shear Capacity of Reinforced Concrete Members," *ACI Structural Journal*, V. 86, No. 5, 1989, pp. 570-581.
- Chak, I. N., "Janus: A Post-Processor for VecTor Analysis Software," M.A.Sc. Thesis, Department of Civil Engineering, University of Toronto, Canada, 2013, 193 pp.
- Collins, M. P., Bentz, E. C., Quach, P., Proestos, G., "The Challenge of Predicting the Shear Strength of Very Thick Slabs," *Concrete International*, V. 37, No. 11, 2015, pp. 29-37.
- Collins, M. P., and Kuchma, D., "How Safe Are Our Large, Lightly Reinforced Concrete Beams, Slabs and Footings?" *ACI Structural Journal*, V. 96, No. 4, 1999, pp. 482-490.
- Collins, M. P., Mitchell, D., Adebar, P., and Vecchio, F. J., "A General Shear Design Method," *ACI Structural Journal*, V. 93, No. 1, 1996, pp. 36-45.
- Collins, M. P., Mitchell, D., and Bentz, E. C., "Shear Design of Concrete Structures," *The Structural Engineer*, V. 86, No. 10, 2008, pp. 32-39.
- Collins, M. P., Vecchio, F. J., and Mehlhorn, G., "An International Competition to Predict the Response of Reinforced Concrete Panels," *Canadian Journal of Civil Engineering*, V. 12, No. 3, 1985, pp. 624-644.
- CSA Committee A23.3, "Design of Concrete Structures," Canadian Standard Association, Rexdale, Ontario, Canada, 2014, 297 pp.
- Deluce, J. R., Lee, S. -C., and Vecchio, F. J., "Crack Model for Steel Fiber-Reinforced Concrete Members Containing Conventional Reinforcement," *ACI Structural Journal*, V. 111, No. 1, 2014, pp. 93-102.
- ElMohandes, F., and Vecchio, F. J., "Reliability of Temperature-Dependent Models for Analysis of Reinforced Concrete Members Subjected to Fire," *ACI Structural Journal*, V. 113, No. 3, 2016, pp. 481-490.
- ElMohandes, F., and Vecchio, F. J., "VecTor3 User's Manual," Department of Civil Engineering, University of Toronto, Toronto, Canada, 2013, 153 pp.
- Elstner, R. C., and Hognestad, E., "Laboratory Investigation of Rigid Frame Failure," *ACI Journal*, V. 53, No. 1, 1957, pp. 637-668.
- Faconi, L., Plizzari, G., and Vecchio, F. J., "Disturbed Stress Field Model for Unreinforced Masonry," *ASCE Journal of Structural Engineering*, V. 140, No. 4, 2014.
- Ferche, A. C., Panesar, D. K., Sheikh, S. A., and Vecchio, F. J., "Toward Macro-Modeling of ASR-Affected Structures," *ACI Structural Journal*, V. 114, No. 5, 2017, pp. 1121-1129.
- Guner, S., and Vecchio, F. J., "Simplified Method for Nonlinear Dynamic Analysis of Shear-Critical Frames," *ACI Structural Journal*, V. 109, No. 5, 2012, pp. 727-737.
- Guner, S., and Vecchio, F. J., "Pushover Analysis of Shear-Critical Frames: Formulations," *ACI Structural Journal*, V. 107, No. 1, 2010, pp. 63-71.
- Gupta, P. R., and Collins, M. P., "Evaluation of Shear Design Procedures for Reinforced Concrete Members under Axial Compression," *ACI Structural Journal*, V. 98, No. 4, 2001, pp. 537-547.
- Habibi, S., "Finite Element Modeling of Corrosion Damaged Reinforced Concrete Structures," M.A.Sc. Thesis, Department of Civil Engineering, University of Toronto, Canada, 2017, 139 pp.
- Hillerborg, A., Mod er, M., and Petersson, P-E., "Analysis of Crack Formation and Crack Growth in Concrete by Means of Fracture Mechanics and Finite Elements," *Cement and Concrete Research*, V. 6, No. 3, 1976, pp. 773-781.
- Hrynyk, T. D., "Behavior and Modeling of Reinforced Concrete Slabs and Shells under Static and Dynamic Loads," Ph.D. Thesis, Department of Civil Engineering, University of Toronto, Canada, 2013, 455 pp.
- Hrynyk, T. D., and Vecchio, F. J., "Modeling of Steel-Concrete Composite Elements under In-Plane and Out-of-Plane Loads," *ASCE Journal of Structural Engineering*, V. 142, No. 10, 2016.
- Hrynyk, T. D., and Vecchio, F. J., "Capturing Out-of-Plane Shear Failures in the Analysis of Reinforced Concrete Shells," *ASCE Journal of Structural Engineering*, V. 141, No. 12, 2015.

- Hunter, M. D., "Towards Stochastic Finite Element Analysis of Reinforced Concrete Structures," M.A.Sc. Thesis, Department of Civil Engineering, University of Toronto, Canada, 2016, 262 pp.
- IA-FraMCoS Conference Proceedings, *Fracture Mechanics of Concrete and Concrete Structures International Conference*, University of California, Berkeley, U.S.A., 2016.
- Isojeh, B., El-Zeghayar, M., and Vecchio, F. J., "Fatigue Behavior of Steel Fiber Concrete in Direct Tension," *ASCE Journal of Materials in Civil Engineering*, V. 29, No. 9, 2017a.
- Isojeh, B., El-Zeghayar, M., and Vecchio, F. J., "Concrete Damage under Fatigue Loading in Uniaxial Compression," *ACI Materials Journal*, V. 114, No. 2, 2017b, pp. 225-235.
- Isojeh, B., El-Zeghayar, M., and Vecchio, F. J., "Simplified Constitutive Model for Fatigue Behavior of Concrete in Compression," *ASCE Journal of Materials in Civil Engineering*, V. 29, No. 7, 2017c.
- Kani, G. N. J., "The Riddle of Shear Failure and Its Solution," *ACI Journal*, V. 61, No. 28, 1964, pp. 441-467.
- Kani, M. W., Huggins, M. W., and Wittkopp, R. R., "Kani on Shear in Reinforced Concrete," Department of Civil Engineering, University of Toronto, Canada, 1979, 225 pp.
- Kim, S. W., and Vecchio, F. J., "Modeling of Shear-Critical Reinforced Concrete Structures Repaired with Fiber-Reinforced Polymer Composites," *ASCE Journal of Structural Engineering*, V. 134, No. 8, 2008, pp. 1288-1299.
- Lee, S. -C., Cho, J. -Y., and Vecchio, F. J., "Analysis of Steel Fiber-Reinforced Concrete Elements Subjected to Shear," *ACI Structural Journal*, V. 113, No. 2, 2016, pp. 275-285.
- Lee, S. -C., Cho, J. -Y., and Vecchio, F. J., "Simplified Diverse Embedment Model for Steel Fiber-Reinforced Concrete Elements in Tension," *ACI Materials Journal*, V. 110, No. 4, 2013a, pp. 403-412.
- Lee, S. -C., Cho, J. -Y., and Vecchio, F. J., "Tension-Stiffening Model for Steel Fiber-Reinforced Concrete Containing Conventional Reinforcement," *ACI Structural Journal*, V. 110, No. 4, 2013b, pp. 639-648.
- Lee, S. -C., Cho, J. -Y., and Vecchio, F. J., "Diverse Embedment Model for Steel Fiber Reinforced Concrete in Tension: Model Development," *ACI Materials Journal*, V. 108, No. 5, 2011, pp. 516-525.
- Loya, A. S., Lourenco, D. D. S., Guner, S., and Vecchio, F. J., "User's Manual of Janus for VecTor5," Department of Civil and Environmental Engineering, University of Toledo, Ohio, U.S.A., 2017, 28 pp.
- Lulec, A., "Simplified Analytical Tools for Impact and Impulsive Loading Analysis of Reinforced Concrete Structures," Ph.D. Thesis, Department of Civil Engineering, University of Toronto, Canada, 2017, 196 pp.
- Mitchell, D., and Collins, M. P., "Diagonal Compression Field Theory-A Rational Model for Structural Concrete in Pure Torsion," *ACI Journal Proceedings*, V. 71, No. 8, 1974, pp. 396-408.
- Montoya, E., "Behavior and Analysis of Confined Concrete," Ph.D. Thesis, Department of Civil Engineering, University of Toronto, Canada, 2003, 321 pp.
- Montoya, E., Vecchio, F. J., and Sheikh, S. A., "Compression Field Modeling of Confined Concrete," *Structural Engineering and Mechanics*, V. 12, No. 3, 2006, pp. 231-248.
- Montoya, E., Vecchio, F. J., and Sheikh, S. A., "Numerical Evaluation of the Behavior of Steel- and FRP-Confined Concrete Using Compression Field Modeling," *J. of Engineering Structures*, V. 26, No. 11, 2004, pp. 1535-1545.
- Mörsch, E., "Concrete-Steel Construction," McGraw-Hill Book Company, New York, U.S.A., 1909, 368 pp.
- Newmark, N. M., "A Method of Computation for Structural Dynamics," *ASCE Journal of the Engineering Mechanics Division*, V. 85, No. 3, 1959, pp. 67-94.
- Palermo, D., and Vecchio, F. J., "Simulation of Cyclically Loaded Concrete Structures Based on the Finite Element Method," *ASCE Journal of Structural Engineering*, V. 133, No. 5, 2007, pp. 728-738.
- Pan, Z., and Li, B., "Truss-Arch Model for Shear Strength of Shear-Critical Reinforced Concrete Columns," *ASCE Journal of Structural Engineering*, V. 139, No. 4, 2013, pp. 548-560.
- Panagiotou, M., Restrepo, J. I., Schoettler, M., and Kim, G., "Nonlinear Cyclic Truss Model for Reinforced Concrete Walls," *ACI Structural Journal*, V. 109, No. 2, 2012, pp. 205-214.
- Polak, M. A., and Vecchio, F. J., "Nonlinear Analysis of Reinforced Concrete Shells," *ASCE Journal of Structural Engineering*, V. 119, No. 12, 1993, pp. 3439-3462.
- Reineck, K., Bentz, E. C., Fitik, B. F., Kuchma, D. A., and Bayrak, O., "ACI-DAfStb Database of Shear Tests on Slender Reinforced Concrete Beams without Stirrups," *ACI Structural Journal*, V. 110, No. 5, 2013, pp. 867-876.
- Saatci, S., and Vecchio, F. J., "Nonlinear Finite Element Modeling of Reinforced Concrete Structures under Impact Loads," *ACI Structural Journal*, V. 106, No. 5, 2009, pp. 717-725.
- Sadeghian, V., "A Framework for Multi-Platform Analytical and Experimental Simulations of Reinforced Concrete Structures," Ph.D. Thesis, Department of Civil Engineering, University of Toronto, Canada, 2017, 321 pp.
- Sadeghian, V., Kwon, O., and Vecchio, F. J., "Modeling Beam-Membrane Interface in Reinforced Concrete Frames," *ACI Structural Journal*, Accepted for publication, 2017a.
- Sadeghian, V., Kwon, O., and Vecchio, F. J., "Small-Scale Multi-axial Hybrid Simulation of a Shear-Critical RC Frame," *Earthquake Engineering and Engineering Vibration*, V. 16, No. 4, 2017b, pp. 727-743.

- Sadeghian, V., and Vecchio, F. J., "Application of Multi-Scale Modeling on Large Shear-Critical Reinforced Concrete Structural Systems Repaired with FRP Sheets," *Innovations in Corrosion and Materials Science*, V. 6, No. 2, 2016, pp. 106-114.
- Sadeghian, V., and Vecchio, F. J., "A Graphical User Interface for Stand-Alone and Mixed-Type Modeling of Reinforced Concrete Structures," *Computers and Concrete*, V. 16, No. 2, 2015, pp. 287-309.
- Sato, Y., and Vecchio, F. J., "Tension Stiffening and Crack Formation in RC Members with FRP Sheets," *ASCE Journal of Structural Engineering*, V. 129, No. 6, 2003, pp.717-724.
- Sherwood, E. G., Bentz, E. C., and Collins, M. P., "Effect of Aggregate Size on Beam-Shear Strength of Thick Slabs," *ACI Structural Journal*, V. 104, No. 2, 2007, pp. 180-190.
- Susetyo, J., Gauvreau, P., and Vecchio, F. J., "Steel Fiber-Reinforced Concrete Panels in Shear: Analysis and Modeling," *ACI Structural Journal*, V. 110, No. 2, 2013, pp. 285-295.
- Trommels, H., "Towards Simplified Tools for Analysis of Reinforced Concrete Structures Subjected to Impact and Impulsive Loading: A Preliminary Investigation," M.A.Sc. Thesis, Department of Civil Engineering, University of Toronto, Canada, 2013, 196 pp.
- Van Mier, J. G. M., "Fracture Processes in Concrete," CRC Press, U.S.A., 1996, 464 pp.
- Vecchio, F. J., "Contribution of NLFEA to the Evaluation of Two Structural Concrete Failures," *ASCE Journal of Performance of Constructed Facilities*, V. 16, No. 3, 2002, pp. 110-115.
- Vecchio, F. J., "Disturbed Stress Field Model for Reinforced Concrete: Formulation", *ASCE Journal of Structural Engineering*, V. 126, No. 8, 2000, pp. 1070-1077.
- Vecchio, F. J., "Finite Element Modeling of Concrete Expansion and Confinement," *ASCE Journal of Structural Engineering*, V. 118, No. 9, 1992, pp. 46-56.
- Vecchio, F. J., "Nonlinear Finite Element Analysis of Reinforced Concrete Membranes," *ACI Structural Journal*, V. 86, No. 1, 1989, pp. 26-35.
- Vecchio, F. J., Bentz, E. C., and Collins, M. P., "Tools for Forensic Analysis of Concrete Structures," *Computer and Concrete*, V. 1, No. 1, 2004, pp 1-14.
- Vecchio, F. J., and Collins, M. P., "Predicting the Response of Reinforced Concrete Beams Subjected to Shear using the Modified Compression Field Theory," *ACI Structural Journal*, V. 85, No. 3, 1988, pp. 258-268.
- Vecchio, F. J., and Collins, M. P., "The Modified Compression-Field Theory for Reinforced Concrete Elements Subjected to Shear," *ACI Structural Journal*, V. 83, No. 2, 1986, pp. 219-231.
- Vecchio, F. J., and Collins, M. P., "Response of Reinforced Concrete to In-Plane Shear and Normal Stresses," Department of Civil Engineering, University of Toronto, Canada, 1982, 332 pp.
- Vecchio, F. J., Lai, D., Shim, W., and Ng, J., "Disturbed Stress Field Model for Reinforced Concrete: Validation," *ASCE Journal of Structural Engineering*, V. 127, No. 4, 2001, pp. 350-357.
- Vecchio, F. J., and McQuade, I., "Towards Improved Modeling of Steel-Concrete Composite Wall Elements," *Journal of Nuclear Engineering and Design*, V. 241, No. 8, 2011, pp. 2629-2642.
- Vecchio, F. J., and Selby, R. G., "Towards Compression Field Analysis of Reinforced Concrete Solids," *ASCE Journal of Structural Engineering*, V. 117, No. 6, 1991, pp. 1740-1758.
- Wagner, H., "Ebene Blechwandträger mit sehr dünnem Stegblech," *Z. Flugtech. Motorluftschiffahrt*, Berlin, Germany, V. 20, No. 8-12, 1929.
- Walraven, J. C., "Fundamental Analysis of Aggregate Interlock," *ASCE Journal of the Structural Division*, V. 107, 1981, pp. 2245-2270.
- Wong, P. S., Trommels, H., and Vecchio, F. J., "VecTor2 and FormWorks User's Manual, 2<sup>nd</sup> Edition," Department of Civil Engineering, University of Toronto, Canada, 2013, 311 pp.
- Wong, P. S., and Vecchio, F. J., "VecTor2 and FormWorks User's Manual," Department of Civil Engineering, University of Toronto, Canada, 2002, 217 pp.